eNeuro

Research Article: Open Source Tools and Methods | Integrative Systems

Development of an open face home cage running wheel for testing activity-based anorexia and other applications

https://doi.org/10.1523/ENEURO.0246-22.2022

Cite as: eNeuro 2022; 10.1523/ENEURO.0246-22.2022

Received: 23 June 2022
Revised: 9 October 2022
Accepted: 10 October 2022

1. Manuscript title: Development of an open face home cage running wheel for testing activity-based anorexia and other applications.

2. Abbreviated title: Open source running wheels

3. Authors: Nathan Godfrey[1], Kehan Chen[1], Temoor Tayyab[1], Gina Dimitropoulos[1], Frank P. MacMaster[1], Stephanie L. Borgland[1]
[1]Hotchkiss Brain Institute
The University of Calgary
3330 Hospital Dr. NW
Calgary, Alberta T2N 4N1

4. Author contributions: N.G., K.C., S.L.B. designed research, N.G., K.C., contributed unpublished analytic tools, N.G., K.C., T.T. performed research, N.G., T.T analyzed data, N.G., S.L.B. wrote the paper, S.L.B, G.D., F.P.M, edited and funded the study.

5. Correspondence should be addressed to: Stephanie L. Borgland
s.borgland@ucalgary.ca

6. Number of Figures: 6 +1

7. Number of Tables: 0

8. Number of Multimedia: 0

9. Number of words for Abstract: 105

10. Nr of words for Significance Statement: 75

11. Number of words for introduction: 461

12. Number of words for discussion: 1389

13. Acknowledgements:
Land acknowledgement:
This work was conceived and performed at The University of Calgary, located on the traditional territories of the people of the Treaty 7 region in Southern Alberta, which includes the Blackfoot Confederacy (including the Siksika, Piikuni, Kainai First Nations), the Tsuut'ina, and the Stoney Nakoda (including the Chiniki, Bearspaw, and Wesley First Nations). The City of Calgary is also home to Metis Nation of Alberta, Region 3.

14: Authors report no conflict of interest.

15: Funding sources: This work was supported by a Mathison Centre for Research and Education research initiative (Finding Treatments for Eating Disorders to GD, FPM, and SLB), an NSERC Discovery grant (DG-343012 / DAS-04060 to SLB) and a Canada Research Chair (950-232211). NG was supported by a Harley N. Hotchkiss Doctoral Scholarship.

Abstract:

Running wheels for mice residing in the home cage are useful for the continuous measurement of locomotor activity for studies testing exercise interventions or exercise-induced effects on brain and metabolism. Here, we have developed an open source, printable, open-faced running wheel that is automated to collect locomotor information such as distance travelled, wheel direction, and velocity that can be binned into epochs over 24 h or multiple days. This system allows for remote data collection to avoid human interference in mouse behavioural experiments. We tested this system in an activity-based-anorexia procedure. Using these wheels, we replicate previous findings that food restriction augments wheel running activity.

Significance statement:

Anorexia Nervosa (AN) is a psychiatric disease with few treatments and a high mortality rate. It is important to better understand the biology to accelerate the development of new therapies. The most used animal model to study AN is the activity-based anorexia model, which measures physical activity during food restriction. We have developed open source running wheels that allow for continuous measurement of activity for multi-day experiments and demonstrated efficacy in the activity-based anorexia model.

Introduction

The prevalence of eating disorders such as anorexia nervosa (AN) has been escalating in recent years (Val-Laillet et al., 2015) and has increased over the covid-19

pandemic (J Devoe et al., 2022). AN has a life-time prevalence of 1 % (Bou Khalil et al., 2017; Hudson et al., 2007; Smink et al., 2012). The mortality rate of these individuals is 5 times greater than a healthy individual (Arcelus et al., 2011; Bou Khalil et al., 2017) which is the highest mortality rate for any mental disorder (Arcelus et al., 2011; Smink et al., 2012; Val-Laillet et al., 2015). Furthermore, the current recovery rate for AN, ten years after onset, is a meager 10% (Bergh et al., 2013). An improved understanding of the etiology and neurobiological underpinnings of this disorder will lead to improved treatments and outcomes.

The hallmark characteristics of AN are a restriction in energy intake that leads to low body weight, an intense fear of gaining weight, and a disturbed body image including over-estimating body size (American Psychiatric Association, 2013). In addition, an increase in physical activity has been observed amongst many individuals with AN (Bergh et al., 2013). A common model used to study AN in rodents is the activity-based anorexia (ABA) model which replicates many symptoms seen in AN (Bergh et al., 2013; Gutierrez, 2013; Routtenberg and Kuznesof, 1968; Watanabe et al., 1992). In this model, access to a running wheel is paired with food restriction, resulting in an increase in activity and a decrease in food consumption and a reduction in body weight. Mice and rats lose the ability to self-regulate their food intake and energy expenditure, eventually resulting in weight loss to the humane endpoint where they are removed from the study.

An important limitation to the ABA model is easy access to mouse running wheels with the ability to record mouse activity. Although commercial products are available, they are expensive and require proprietary software devoted to wheel use (Welch et al., 2018). Many commercial products also use a closed wheel that is not compatible with modern optical and recording techniques. Other open source wheel designs had features that were not ideal for our application (Bivona and Poynter, 2021; Zhu et al., 2021). For these reasons, we designed and constructed an open source running wheel system that runs independent from a central computer. The wheels are 3D printed and are operated using a Raspberry Pi zero W, a small but highly available microprocessor, and are programmed in Python. The data are transmitted to a personal computer via email, where it is then automatically downloaded, parsed, and analyzed with Python and MATLAB programs. Our running wheel system is inexpensive, simple, adaptable, and completely open source. In this study, we demonstrated its utility with the ABA model.

Methods

Mice

32 Female BALB/c mice (Charles River; Trois Riviere, QC) 7-8 weeks old were used for the ABA model. Mice acclimatized in the animal facility 3-5 days before the habituation period of the study. Prior to habituation, mice were housed in groups of 2-5, maintained on a 12 h light-dark schedule (lights on at 08.00 h, zeitgeber time (ZT) 0), and given chow and water *ad libitum*. Mice were fed standard chow (5062 from Pico-Vac lab diet, Lab Supply, Fort Worth Tx), which is composed of (% of total kcal) 23% protein, 22% fat

(ether extract), and 55% carbohydrate. The total density of this diet was 4.60 kcal g^{-1}. All experiments and procedures were in accordance with the ethical guidelines established by the Canadian Council for Animal Care and were approved by the University of Calgary Animal Care Committee (protocol no. AC21-0034).

Running Wheels

Each running wheel consists of a 3D printed wheel and electrical components connected to a Raspberry Pi 0 W (Figure 1a) (www.PiShop.ca). The spinner part of the wheel contains a metal ball bearing at the centre and is surrounded by three sets of magnets that are evenly spaced. Three hall effect sensors that protrude up through the wheel's base detect changes in the magnetic field, which occurs when the magnets pass over top. Each hall effect sensor has three pins, with the first pin being connected to the 3.3 V Raspberry Pi power supply through the MCP3008 analog digital converter (ADC) (Figure 1A,B). The second pin connects to the Raspberry Pi ground. The third pin transmits magnetic field values to the Raspberry Pi through the ADC. To reduce noise, a 10 kΩ pull-up resistor is placed between the third pin and ground. The ADC is soldered to a piece of PCB prototyping board and 20-gauge solid wires connect the board to the Raspberry Pi and the three hall effect sensors. The three hall effect sensors are inserted inside a 3D printed sensor holder, which fits through a gap left in the base of the wheel. All Raspberry Pi's receive power through the micro-USB port. Copper tubing was bent and cut to serve as a protective sleave for the USB power cable inside of the mouse cage. The total cost of each wheel was approximately $65.00 CAD.

136

137 3D Printing

138 All files for spinner parts were made as SLDPRT in solid works and then
139 converted to STL files. Both SLDPRT and STL files are available at
140 (https://github.com/borglandlab/RunningWheel) to allow for direct printing or modifying
141 the wheel to individual needs. When assembled the wheel is width: 15.24 cm (6 inches),
142 height: 10.64 cm (4.19 inches), and depth: 14.45 cm (5.69 inches). Using the STL files,
143 3D models were then sliced using Cura 4.9 in preparation for printing
144 (https://ultimaker.com/learn/ultimaker-cura-4-9-seamless-and-efficient-with-digital-
145 library-integration). For the wheels used in the ABA model, printing was done using
146 either a Stock Eryone Thinker ER20 (ShenZhen Eryone Technology Co., Ltd,
147 Shenzhen, China) or FLSUN QQ-S-pro (Zhengzhou Chaokuo Electronic Co., Ltd,
148 China) with 0.4 mm E3D V6 nozzle. All 3D printing used generic 1.75 mm diameter
149 PLA. To demonstrate the universal nature of our design, all wheel parts were also sliced
150 and printed with the Sindoh 3DWOX printer (Sindoh Co., Ltd, Seoul, Korea) and
151 supporting software with excellent results. More information on the printing process can
152 be found within our 3D model files.

153

154 Raspberry Pi Code

155 The Raspberry Pi is programmed to continuously check the values of all three
156 hall effect sensors. When the value of one hall effect sensor is greater than 30, the
157 trigger time and values for all three hall effect sensors are recorded. New values cannot
158 be recorded until the values for all three hall effect sensors drop below 15, allowing the

magnet to clear to ensure that the next trigger is indeed a separate incident. Thus, a single magnet passing over the three sensors will not accidently trigger the sensors more than once. For this reason, because there are magnets in three different locations on the spinner top, each triggering of the hall effect sensors reliably indicates that the mouse has travelled one third of the circumference at the running position of the spinner top. Every hour, or when the number of recorded entries is greater than 3000, the entries are written to a text file. This data will be stored on the micro-SD card and can be accessed at the end of the experiment. Even though writing to the text file is relatively fast, the Raspberry Pi will wait for a moment when no wheel movement is occurring to ensure that minimal data is lost during this process. In addition, if the Raspberry Pi detects an internet connection with speeds greater than 1 Mb/s it will also send an email containing the text file information to the specified email account. The frequency of how often data will be stored and transmitted can be adjusted for specific experimental needs (Figure 1A). To connect the Raspberry Pis to the university network, we supplied the MAC addresses from each Raspberry Pi to the IT services.

Personal Computer

Using Python code (https://github.com/borglandlab/RunningWheel), the emails sent from the Raspberry Pi are downloaded (Figure 1A,B). Trigger times and values for each hall effect sensor are parsed from the text, organized, and stored in a MS Excel workbook. Individual emails are stored as sheets within a workbook, with a maximum of 49 sheets per workbook before a new workbook is created. Each running wheel is assigned a folder that will contain all the excel workbooks for that specific wheel. A

directory MS Excel workbook is also created to keep track of the location of each sheet. A MATLAB program imports the data from these excel workbooks and stores each individual time point, direction of wheel rotation, the cumulative distance, and the velocity for all running wheels in a MATLAB structure (www.Mathworks.com). MATLAB will also immediately create graphs showing the total distance and average velocity of the wheels. This code is run from a Python GUI (www.Python.org); automatically taking the data from a text file in your email account to an organized MATLAB structure and viewable graphs. The MATLAB structure can be further analyzed by the code provided or by your own personal analysis. Furthermore, data can be binned into daily and hourly time frames, making analysis and data visualization more versatile (Figure 1).

In addition to data collected from the running wheel, we also recorded body weight, food and water weight each day on a workbook stored in Dropbox (www.Dropbox.com). This allowed us to automatically calculate changes in mouse weight, change in food and water consumption, and the removal from study threshold with MATLAB. Graphs were automatically generated. Like the code for the running wheel, this can also be run from our Python GUI. However, because this code is specific to our experiment, it has been made optional to run in the experiment.

Activity-based anorexia model (ABA)

The ABA model used in this study was based on models previously published (Achamrah et al., 2017; Ho et al., 2016; Welch et al., 2018). Mice were placed in individual cages that contained a spinning or non-spinning (dummy) running wheel, cardboard shelter, water bottle, and ad-libitum chow in a feeding hopper and left

uninterrupted for 48 h to habituate to the novel cage. A 7-day baseline period immediately followed the habituation period. During the baseline, bodyweight, food, and water, were weighed each day at ZT 01.30 h. The spinner tops were cleaned, and 8-10 g of new food was weighed and left in the food hopper. Following baseline, mice were split into four groups: 1) *ad libitum* with dummy wheel (n = 8), 2) *ad libitum* with running wheel (n = 8), 3) food restricted with dummy wheel (n = 8), and 4) food restricted with running wheel (n = 8). Group 1 was paired with group 3, and group 2 was paired with group 4, such that measurements could be compared to a time-matched control. During this period, groups 3 and 4 were given access to food for 6 hrs (ZT 01.30 h – ZT 07.30 h) for 3 days (days 8-10). In a pilot study, mice did not lose weight to the humane endpoint when on 6h restriction for up to 10 days (Figure 2-1 supporting Figure 2B), therefore we modified the protocol so that after 3 days of 6h restriction, they were food restricted to 3h (ZT 01.30 h – ZT 04.30 h) for the next 6 days (days 11 to 17, Figure 2A). Body weight, food, and water were weighed daily at ZT 01.30 h. Spinner tops were cleaned at ZT 01:30h for non-restricted mice, and after food restriction for restricted mice. Restricted mice, and their paired controls, were removed from the study if their body weight fell to 75% of their body weight recorded on the last day of baseline. Daily measurements of distance and velocity were recorded from ZT 17.00 h (12:00 AM) to ZT 17.00 h the next day. The anticipatory activity was measured in the 3 hours prior to food access. Activity during food intake was measured during first 3 hours of food access. Activity during the post-prandial period was measured ZT 07.30 h to ZT 10.30 h. Mice begin to be removed from the experiment during day 11 and by day 13, after 6

227 days of food restriction, only one mouse remained in groups 2 and 4, obscuring
228 comparisons beyond this point.
229
230 **Data Analysis**
231 All values are expressed as means +/- SEM and assessed for normality using a
232 Shapiro-Wilk test. Statistical significance was assessed by using two-tailed unpaired
233 Student's t test for two comparisons. A two-way ANOVA followed by Sidak's multiple
234 comparisons was used for multiple group comparisons. GraphPad Prism 8.3 (GraphPad
235 Software, Inc., La Jolla, CA, USA) was used to perform statistical analysis.
236
237 **Results**
238 To validate the utility of our 3D printed running wheels, we carried out a 3-week
239 long activity-based anorexia (ABA) model. During the 7-day baseline period, mice had
240 access to active or inactive (dummy) running wheels and *ad libitum* access to food and
241 water. On the final day of baseline, body weight was compared across the 4 groups: *Ad*
242 *lib* dummy (17.7 ± 0.2 g), *Ad lib* wheel (17.4 ± 0.3 g), food restriction (FR) dummy (17.7
243 ± 0.3 g), FR wheel (18.0 ± 0.3 g). There was no main effect of wheel running or food on
244 body weight (running effect: $F(1, 28) = 0.003$, $P=0.9$; food effect: $F(1, 28) = 1.0$, $P=0.3$)
245 or wheel running x food interaction (interaction: $F(1, 28) = 0.8$, $P=0.4$).
246 To examine the effect of FR on body weight, food and water consumption, and
247 wheel running we measured these parameters on day 11, the first day of the second
248 restriction phase. This was the timepoint when some mice first reached the humane
249 endpoint and removal from the study. The number of days to reach the humane

endpoint whereby mouse body weight dropped to 75% of their body weight from that measured on the last day of baseline was compared between FR exposed to wheel running and FR with a dummy wheel. FR mice exposed to wheel running had reduced probability of survival compared to FR mice with the dummy wheel (Log-rank test: X^2= 5.1, Df = 1, P = 0.02; Figure 2B). Thus, FR mice with access to a running wheel are removed from the experiment earlier.

To determine the effect of FR, mouse body weight was compared between groups on day 11. FR wheel mice were 78.1 ± 1.5% of their baseline body weight whereas *Ad lib* dummy was 99.7 ± 0.9%, *Ad lib* wheel was 100 ± 0.8%, and FR dummy was 91.7 ± 1.9% of their original body weight. There were main effects of running and FR (running effect: F(1, 28) = 9.8, P<0.004; restriction effect: F(1, 28) = 40.9, P<0.0001) as well as a running x FR interaction (interaction: F(1, 28) = 7.3, P= 0.01). A Sidak's multiple comparisons test showed that FR wheel mice lost more weight than FR dummy mice (P=0.002), and *Ad lib* wheel mice (P<0.0001; Figure 3A,B).

Daily food consumption was compared between groups (Figure 3C,D). 24h food consumption from day 10 demonstrated a main effect of FR (restriction effect: F(1, 28) = 34.6, P<0.0001) but no effect of running (running effect: F(1, 28) = 3.4, P= 0.07) on food consumption. Given that both wheel and dummy groups had reduced food consumption during the FR period, there was no interaction (F(1,28) = 0.2, P= 0.7). However, a Sidak's posthoc on the main effect of restriction indicated significant reductions in food intake in both dummy (*Ad Lib* Dummy: 3.1 ± 0.3 g vs FR Dummy: 1.7 ± 0.2 g; P = 0.0002) and running wheel groups (*Ad Lib* Wheel: 3.4 ± 0.2 g vs FR Wheel: 2.2 ± 0.2 g;

P = 0.001; Figure 3D). Thus, access to the running wheel did not further restrict food intake in the FR group.

We next measured daily water consumption (Figure 3E, F). On Day 10, there was a main effect of FR on 24h water consumption (restriction effect: $F(1, 28) = 46.4$, $P<0.0001$) but no effect of running on water consumption (running effect: $F(1,28) = 3.9$, $P = 0.06$) or running x FR interaction (interaction: $F(1,28) = 0.1$, $P = 0.7$). A Sidak's posthoc on the main effect of restriction indicated a significant increase in water intake in both dummy (*Ad Lib* Dummy: 4.1 ± 0.2 mL vs FR Dummy: 6.4 ± 0.3 mL, $P <0.0001$) and wheel running groups (*Ad Lib* Wheel: 4.8 ± 0.3 mL vs FR Wheel: 6.9 ± 0.5 mL, $P = 0.0002$; Figure 3F). Taken together, these data indicate that FR mice with access to a running wheel have reduced body weight compared to FR mice without the running wheel. However, food and water intake between these groups was similar.

We next recorded daily 24 h locomotor activity of *Ad lib* and FR mice with access to our 3D printed running wheels and supporting Python/MATLAB code (Figure 4). Distance traveled between *Ad Lib* and FR mice was measured daily. There were 8 mice per group until Day 11 when mice were removed from the study due to low body weight, and thus the number of animals per group varied on subsequent days (day 11: n = 6, day 12-16: n = 1; Figure 4A). Thus, averaged distance traveled during restriction was measured the morning of Day 11 which accounted for the preceding 24h period prior to mice being removed from the study. There was a main effect of restriction ($F(1,28) = 21.1$, $P<0.0001$) and a main effect of time ($F(1,28) = 12.5$, $P = 0.001$) and a time x

restriction interaction ($F(1,28) = 12.5$, $P = 0.001$). A Sidak's post hoc test indicated no difference during the baseline period (Day 7) but a significant increase in distance travelled after food restriction ($P< 0.0001$, *Ad Lib*: 7.7 ± 1.2 km vs FR: 22.5 ± 3.0 km; Figure 4B). Thus, FR increases wheel running in mice.

We next examined if FR influences daily anticipatory activity in the 3h period prior to food delivery (Figure 4C,D). There was a main effect of restriction ($F(1,28) = 8.2$, $P= 0.008$) and a main effect of time ($F(1,28) = 16.5$, $P= 0.0003$), and a significant restriction x time interaction ($F(1,28) = 5.2$, $P = 0.03$). A Sidak's posthoc test indicated no significant difference during baseline (day 7; $P = 0.9$), but a significant increase in anticipatory activity during restriction (day 11; *Ad Lib*: 0.9 ± 0.4 km vs FR: 2.8 ± 0.4 km; $P = 0.002$; Figure 4D). Thus, FR increases anticipatory wheel running.

Activity during the first 3h of the food availability period was not different between groups (Ad lib wheel: 0.6 ± 0.2 km, FR wheel: 0.4 ± 0.1 km). There was no main effect of restriction ($F(1, 28) = 0.2$, $P = 0.6$) or time ($F(1,28) = 2.0$, $P = 0.2$) or restriction x time interaction ($F(1,28, 0.04)$, $P = 0.8$; Figure 4E,F). These results suggest that, in our procedure, FR mice are making choices for food over wheel running during food availability.

We next examined daily wheel running activity during the postprandial period (Figure 4G). There was a main effect of restriction ($F(1,28) = 7.9$, $P = 0.009$) and a main effect of time ($F(1,28) = 10.5$, $P = 0.003$) and a significant restriction x time interaction ($F(1,28) = 7.1$, P 0.01). A Sidak's post hoc test indicated that while post-prandial activity was not different between groups during the baseline ($P = 0.99$), in the 3h period after food access, the post-prandial activity was greater in FR mice (3.1 ± 0.7 km) than *Ad lib*

318 mice (0.7 ± 0.3 km, P=0.001; Figure 4H). Thus, FR mice increase their activity in the
319 period after food availability compared to *Ad Lib* mice.
320 To examine the circadian pattern of activity, we compared hourly distance
321 traveled of *Ad Lib* or FR mice binned by hour and plotted across all of day 10, from
322 12:00AM day 10 to 12:00AM day 11. There was a main effect of restriction ($F(1,14) = 20.9$, $P = 0.0004$), a main effect of time ($F(4.06,58.84) = 13.05$, $P < 0.0001$) and a time x
323 restriction interaction ($F(23,322) = 4.03$, $P < 0.0001$). A Sidak's posthoc test revealed
324 significant differences in activity between *Ad lib* and FR groups in hours 18-24, the early
325 part of their dark cycle (Figure 5A). Furthermore, to demonstrate the full utility of the
326 running wheels, total daily activity of both *Ad lib* and restricted mice was plotted,
327 showing the direction of the rotation of the wheels (i.e., clockwise (CW) or counter
328 clock-wise (CCW); Figure 5B-C). We recorded wheel rotations in CW or CCW from *Ad*
329 *Lib* and FR mice, with a greater amount of running in the CCW wheel direction. Taken
330 together, FR mice travel greater distances on the running wheels over a 24 h period.
331
332 Given the high sensitivity of these running wheels, we calculated the average
333 daily velocity of the mice from the recorded data (Figure 6A). When comparing the
334 baseline (day 7) to the final day before some mice were removed from the study (day
335 11), we found a main effect of restriction ($F(1,28) = 8.9$, $P = 0.006$), but no main effect of
336 time ($F(1,28) = 0.2$, $P = 0.7$) or a significant time x restriction interaction ($F(1,28) = 1.7$,
337 $P = 0.2$). We performed Sidak's posthoc tests on the main effect of restriction and found
338 no significant difference on the baseline day 7 (Ad lib: 1.7 ± 0.1 km/h vs FR: 1.8 ± 0.1
339 km/h; $P = 0.4$), but a significant increase in velocity after restriction (Ad lib: 1.5 ± 0.1
340

km/h vs FR: 2.1 ± 0.2 km/h; P = 0.01; Figure 6B). Similarly, for the 3h anticipatory velocity, there was a main effect of restriction ($F(1,28) = 10.1$, $P = 0.004$), but no main effect of time ($F(1,28) = 0.04$, $P = 0.8$) or a time x restriction interaction ($F(1,28) = 2.3$, P 0.1). A Sidak's post hoc test on the main effect of restriction revealed a significant difference after FR (Ad lib: 1.1 ± 0.2 km/h vs FR: 1.9 ± 0.2 km/h; P = 0.005), but not during baseline (Ad lib: 1.4 ± 0.2 km/h vs FR: 1.7 ± 0.1 km/h; P = 0.4; Figure 6C,D). During the food availability period, there were no main effects of restriction ($F(1,28) = 3.3$, $P = 0.08$), or time ($F(1,28) = 2.2$, $P = 0.2$), or restriction x time interaction ($F(1,28) = 0.7$, $P = 0.4$; Ad lib: 1.4 ± 0.1 km/h vs FR: 1.5 ± 0.1 km/h; Figure 6E,F). Finally, during the 3h post-prandial period, there was no main effects of restriction ($F(1,28) = 0.001$, P = 0.9) or time ($F(1,28) = 4.1$, $P = 0.05$) on velocity (Ad lib: 2.0 ± 0.2 km/h vs FR: 1.5 ± 0.1 km/h; Figure 6G,H). Taken together, this running wheel platform can also provide measurements of velocity and we demonstrate that FR mice also have increased velocity during the anticipatory period.

Discussion

Our team has designed and built an open source running wheel system and validated the utility of our system through the activity-based anorexia (ABA) model. There are several advantages to our running wheels. First, they are highly economical in comparison to commercial products. The total cost to produce our wheels is approximately $65 CAD and uses components that are readily available. This also means that replacement parts can be made should mice damage a part during the experiment. Second, the design of our running wheels makes them suitable for a variety

of experiments and cage types. Like commercial and other opensource products, these wheels have a low-profile design, making them ideal for mouse cages with low lids. Also, due to the open top design of the spinner these wheels are compatible with both optogenetics and fiber photometry. Third, with three sensors and three magnet locations, our running wheels can be used to reliably monitor the distance run by mice and monitor details such as wheel direction and speed. This increases their utility as a tool for data collection. Fourth, this system is adaptable for any lab without the need for an expensive computer and software for operation and data acquisition. These wheels only need power and an internet connection. Even a good internet connection has moments of instability, therefore these running wheels are built with safeguards to test the internet connection before downloading data. The activity of the mice can then be monitored using our Python and MATLAB programs on your personal computer so that the experimenter is not in the room influencing the activity of the mice. Fifth, these running wheels can be replicated even without advanced expertise in electronics and computer science. All wheel parts are print-ready. However, we have included SLDPRT files which can be modified to your specific application. Although soldering is required for connecting the electrical components, the use of the PCB prototyping board makes this process straightforward. In addition, all the code to run this system, from the Raspberry Pi to your personal computer, is written in either Python or MATLAB, making this system adaptable to fit your specific needs. Furthermore, versions of this code are provided for both macOS and Windows operating systems.

Our running wheels have three limitations that are the result of design choices made to improve utility. First, our running wheels are not battery powered like some commercial products, but instead require connection to a USB power cable. This choice was made to avoid the need for battery changes throughout a long-term experiment, which we felt would become more disruptive. Our ABA protocol lasts for about 3 weeks. Avoiding the problem of dead batteries also avoids the potential of lost data. In addition, using an external power supply also allowed us to design a system that favors data collection speed and precision over energy efficiency. The USB power cable allows for utility despite the battery limitation.

Second, an added feature of our running wheels is their ability to autonomously collect and transfer data via email in addition to saving the data to an SD card. This design removes the need for a nearby computer to act as a hub for data collection. However, according to our tests, this design requires a reliable internet connection and internet speeds of 1 mb/s or greater for transmitting data via email. However, if the internet connection drops below 1 mb/s, we have programmed a fail-safe, such that our running wheels will determine if the internet speed is greater than 1 mb/s before attempting to transmit an email. If the internet speed is too slow, the data will only be saved to the SD card and no email will be sent. This is essential since attempting to transmit an email when the internet speed is too slow can result in the system freezing and data collection being interrupted. In most circumstances, this safeguard will prevent the Raspberry Pi from freezing. For the rare occurrence that the Raspberry Pi either freezes or becomes disconnected from the power source, our data download code also checks to see if an email has been sent from each running wheel in the past 3 hours,

409 sending an alert email to your personal email if this has not occurred. However, even
410 with these safeguards in place, if the internet connection is unreliable or slower than 1
411 mb/s, we recommend using the no-Wi-Fi version of the spinner code that we have
412 provided.

413 Third, our running wheels do not transfer data in real-time. This means that,
414 without modifications, they are not designed to be used if your need is to visualize
415 mouse activity each second as it happens. In our design, the running wheel instead
416 sends data either after one hour or when the stored file reaches a specified capacity of
417 3000 entries. We found that this approach was more reliable in long-term multi-day
418 experiments. Taken together, our design is intended for long-term data collection of
419 mouse activity with hourly data visualization.

420 Similar to other low-cost open source running wheel options (Bivona and
421 Poynter, 2021; Edwards et al., 2021; Mayr et al., 2020; Zhu et al., 2021), our systems
422 offers a small, low profile wheel compatible with almost any murine cage (our facility
423 uses Techniplast's Green Line cages) and data storage on microSD cards that tracks
424 distance, running time, and velocity. Using a magnet and hall effect sensors appears to
425 be a common mechanism to record wheel movement (Bivona and Poynter, 2021;
426 Edwards et al., 2021; Mayr et al., 2020), although some designs have employed a
427 magnet detected by a reed switch (Zhu et al., 2021). With 3 hall effect sensors we, and
428 others (Bivona and Poynter, 2021; Mayr et al., 2020), are able to record wheel
429 directionality. Other wheels have features that we did not require for our experiments,
430 such as wheel locking to limit running activity (Edwards et al., 2021; Mayr et al., 2020),
431 an RFID reader (Mayr et al., 2020), as our experiments required unlimited running and

individual housing with food restriction. Further, we employed a wired power set up as we were concerned about battery failure in the long duration of our experiments. Although other systems claimed that the lithium batteries could last up to a month, this was not tested directly (Zhu et al., 2021). One critical difference with our system compared to others is that we used a low cost Raspberry Pi single board computer instead of microcontrollers such as an Adafruit feather (Zhu et al., 2021) or Arduinos (Bivona and Poynter, 2021; Edwards et al., 2021; Mayr et al., 2020). While those systems have reduced power draw, the Raspberry Pi offers increased flexibility in customizability and programmability using common programming languages, such as Python. Taken together, there are a variety of open source running wheels available that have their advantages and disadvantages. Our system offers another option with increased flexibility in programming.

To verify that this application works using the ABA model, we have demonstrated that consistent with other studies, FR mice have increased distance travelled, anticipatory, and post-prandial locomotor activity compared to the non-restricted control mice (Beeler and Burghardt, 2021; Chowdhury et al., 2015; Klenotich and Dulawa, 2012). While this did not alter self-induced food restriction, it did lead to a greater weight loss that restricted controls suggesting that they could no longer match their food intake with their energy needs. Our model used a progressive restriction of food availability. This method allowed for prolonging the activity of mice in our experiment and to delay the severe reductions in activity due to a loss of energy requirements. Given the reductions in quality of life, high mortality rate and lack of effective treatments for AN,

new models, such as ours, are needed to explore the neurobiological underpinnings of this disease and to identify novel therapeutic targets.

In conclusion, we have developed a running wheel and running wheel system that is open-source, economical, and highly versatile. Access to these running wheels will increase the ability of other labs to do research on AN, leading to improved treatments and outcomes. In addition, there are numerous additional experiments where these wheels can be implemented. Running wheel activity can be used to assess stress, hyperactivity, exercise induced plasticity, and disruptions in circadian cycles. All of these are important aspects of numerous mental illnesses, increasing the translatability of experimental results.

References:

Achamrah N, Nobis S, Goichon A, Breton J, Legrand R, do Rego JL, do Rego JC, Déchelotte P, Fetissov SO, Belmonte L, Coëffier M (2017) Sex differences in response to activity-based anorexia model in C57Bl/6 mice. Physiology and Behavior 170:1–5.

American Psychiatric Association (2013) Diagnostic and statistical manual of mental disorders, 5th ed.

Arcelus J, Mitchell AJ, Wales J, Nielsen S (2011) Mortality rates in patients with anorexia nervosa and other eating disorders: A meta-analysis of 36 studies. Archives of General Psychiatry 68:724–731.

Beeler JA, Burghardt NS (2021) Activity-based Anorexia for Modeling Vulnerability and Resilience in Mice. Bio Protoc 11:e4009.

Bergh C et al. (2013) Effective treatment of eating disorders: Results at multiple sites. Behavioral Neuroscience 127:878–889.

Bivona JJ, Poynter ME (2021) An open-source, lockable mouse wheel for the accessible implementation of time- and distance-limited elective exercise. PLoS One 16:e0261618.

Bou Khalil R, Souaiby L, Farès N (2017) The importance of the hypothalamo-pituitary-adrenal axis as a therapeutic target in anorexia nervosa. Physiology and Behavior 171:13–20.

Chowdhury TG, Chen Y-W, Aoki C (2015) Using the Activity-based Anorexia Rodent Model to Study the Neurobiological Basis of Anorexia Nervosa. J Vis Exp e52927.

Edwards J, Olson B, Marks DL (2021) Constructing and programming a cost-effective murine running wheel with digital revolution counter. Lab Anim (NY) 50:202–204.

Gutierrez E (2013) A rat in the labyrinth of anorexia nervosa: Contributions of the activity-based anorexia rodent model to the understanding of anorexia nervosa. International Journal of Eating Disorders 46:289–301.

Ho E V., Klenotich SJ, McMurray MS, Dulawa SC (2016) Activity-based anorexia alters the expression of BDNF transcripts in the mesocorticolimbic reward circuit. PLoS ONE 11:1–15.

Hudson JI, Hiripi E, Pope R. HG, Kessler RC (2007) The Prevalence and Correlates of Eating Disorders in the National Comorbidity Survey Replication. Biological Psychiatry 61:348–358.

J Devoe D, Han A, Anderson A, Katzman DK, Patten SB, Soumbasis A, Flanagan J, Paslakis G, Vyver E, Marcoux G, Dimitropoulos G (2022) The impact of the COVID-19 pandemic on eating disorders: A systematic review. Int J Eat Disord.

Klenotich SJ, Dulawa SC (2012) The activity-based anorexia mouse model. Methods Mol Biol 829:377–393.

Mayr KA, Young L, Molina LA, Tran MA, Whelan PJ (2020) An economical solution to record and control wheel-running for group-housed mice. J Neurosci Methods 331:108482.

Routtenberg A, Kuznesof AW (1968) “Self-Starvation” of Rats Living in Activity Wheels: Adaptation Effects. Journal of Comparative and Physiological Psychology 66:234–238.

Smink FRE, Van Hoeken D, Hoek HW (2012) Epidemiology of eating disorders: Incidence, prevalence and mortality rates. Current Psychiatry Reports 14:406–414.

Val-Laillet D, Aarts E, Weber B, Ferrari M, Quaresima V, Stoeckel LE, Alonso-Alonso M, Audette M, Malbert CH, Stice E (2015) Neuroimaging and neuromodulation approaches to study eating behavior and prevent and treat eating disorders and obesity. NeuroImage: Clinical 8:1–31.

Watanabe K, Hara C, Ogawa N (1992) Feeding conditions and estrous cycle of female rats under the activity-stress procedure from aspects of anorexia nervosa. Physiology and Behavior 51:827–832.

Welch AC, Katzka WR, Dulawa SC (2018) Assessing activity-based anorexia in mice. Journal of Visualized Experiments 2018:1–11.

Zhu M, Kasaragod DK, Kikutani K, Taguchi K, Aizawa H (2021) A Novel Microcontroller-Based System for the Wheel-Running Activity in Mice. eNeuro 8:ENEURO.0260-21.2021.

Figure legends:

Figure 1. Description of the running wheels and computer interface. **A.** Illustration indicating how data is collected and distance and velocity are calculated. **B.** Illustration of the Raspberry Pi motherboard connections. Image of the Raspberry Pi computer is adapted from https://en.wikipedia.org/wiki/Raspberry_Pi. **C.** Photo of a mouse on the running wheel when connected to a fibre optic patch cord. **D.** Photo of a Green Line cage containing a mouse on the wheel with the power cord attached through the bottle holder. Water bottles are delivered via the food hopper for these experiments. Additional photos of the wheel are located at: https://github.com/borglandlab/RunningWheel.

Figure 2. Mice on an activity-based anorexia model with access to a running wheel have decreased probability of survival when food restricted. **A.** Description and time course of the 4 groups; 1) *Ad lib* + dummy, 2) *Ad lib* + wheel, 3) FR + dummy, 4) FR + wheel. **B.** FR mice with access to a running wheel (red) are removed from the study sooner when food restricted compared to *Ad lib* mice with a running wheel (black). Extended data 2-1 indicates that mice did not lose weight to the humane endpoint when on 6h restriction for up to 10 days. As such we added a 3h restriction after 3 d of 6h restriction.

Figure 3. FR Mice with access to a running wheel lose more body weight. **A.** Time course of daily body weight measurements taken at 9 am each day during baseline, 6h food restriction and then 3 hr food restriction. **B**. Bodyweight measurements from *Ad lib* (open bars) or FR (filled bars) mice with access to a dummy wheel or running wheel on Day 11, the time point before some mice were removed from the study. **C**. Time course

554 of food consumption each day during baseline, after the 3 h FR period or after the 6 h
555 FR period. **D.** Food intake over the 24h period preceding the time point before some
556 mice were removed from the study from *Ad lib* (open bars) and FR (filled bars) mice. **E**.
557 Daily water consumption during baseline, 3h FR and 6h FR. FR increased water
558 consumed in both groups regardless of access to the running wheel. **F.** Water
559 consumption over the 24h period preceding the time point before some mice were
560 removed from the study from *Ad lib* (open bars) and FR (filled bars) mice that have
561 access to a dummy or running wheel. Bars represent mean ± S.E.M. Symbols
562 represent individual mice.
563
564 **Figure 4.** Distance traveled increases with food restriction. **A**. Daily distance travelled
565 on the running wheel in *Ad lib* (open circles) or FR (filled circles) mice. **B.** Averaged
566 distance travelled over 24h measured on day 7 or day 11 from *Ad lib* (open bars) or FR
567 (filled bars) mice. **C**. Daily anticipatory activity measured within the 3h period before
568 food delivery in *Ad lib* or FR mice. **D**. Averaged 3h anticipatory activity measured on
569 day 7 or day 11 from *Ad lib* (open bars) or FR (filled bars) mice. **E.** Daily distance
570 travelled measured during the 3h food availability period from *Ad lib* or FR mice. **F**.
571 Averaged distance traveled during the first 3h of the food availability period on day 7 or
572 day 11 from *Ad lib* or FR mice. **G**. Time course of daily postprandial activity over 3h
573 after food access from *Ad lib* or food restricted mice. **H.** Averaged 3h postprandial
574 distance traveled on day 7 or day 11 from *Ad lib* or FR mice. Bars represent mean ±
575 S.E.M. Symbols represent individual mice.
576

Figure 5. Circadian pattern of wheel running. **A.** Over a 24 h period, hourly wheel running is enhanced in FR mice (filled circles) compared to *Ad lib* mice (open circles) except during the food availability period. This data was recorded on day 10. Shaded boxes represent the dark cycle. Hashed lines represent the food availability period. **B.** Daily wheel running in *Ad lib* mice on day 10 as identified by clockwise running (open bars) and counter-clockwise running (filled bars). **C.** Daily wheel running in FR mice on day 10 as identified by clockwise running (open bars) and counter-clockwise running (filled bars). Bars represent mean ± S.E.M. Symbols represent individual mice.

Figure 6. Averaged velocity is greater in FR mice. A. Daily velocity on the running wheel in *Ad lib* (open circles) or FR (filled circles) mice. **B.** Averaged velocity over 24h measured on day 7 or day 11 from *Ad lib* (open bars) or FR (filled bars) mice. **C**. Daily velocity measured within the 3h period before food delivery in *Ad lib* or FR mice. **D**. Averaged 3h anticipatory velocity measured on day 7 or day 11 from *Ad lib* (open bars) or FR (filled bars) mice. **E.** Daily velocity measured during the 3h food availability period from *Ad lib* or FR mice. **F**. Averaged velocity during the first 3h of the food availability period on day 7 or day 11 from *Ad lib* or FR mice. **G**. Time course of daily postprandial velocity over 3h after food access from *Ad lib* or food restricted mice. **H.** Averaged 3h postprandial velocity on day 7 or day 11 from *Ad lib* or FR mice. Bars represent mean ± S.E.M. Symbols represent individual mice.

Extended data Figure 2-1 supporting Figure 2. FR Mice with access to a running wheel lose body weight but adapt food intake. **A.** Time course of daily body weight

measurements taken at 9 am each day during baseline, 6h food restriction. **B**. Bodyweight measurements from *Ad lib* (open bars, n = 4) or FR (filled bars, n = 4) mice with access to a dummy wheel or running wheel on Day 11, the time point before one mouse was removed from the study due to dermatitis. Bodyweight was less in restricted mice ($t(6) = 4.13$, $P = 0.0061$). **C**. Time course of food consumption each day during baseline, after the 6h FR period. **D.** Food intake over the 24h period on day 11 from *Ad lib* (open bars, n = 4) and FR (filled bars, n = 4) mice was decreased in restricted mice ($t(6) = 4.65$, $P = 0.0035$). **E**. Daily distance travelled on the running wheel in *Ad lib* (open circles, n = 4) or FR (filled circles n= 4) mice. **F.** Averaged distance travelled over 24h measured on day 11 from *Ad lib* (open bars) or FR (filled bars) mice was not different between groups ($t(6) = 2.4$, $P = 0.053$). Bars represent mean $\pm$ S.E.M. Symbols represent individual mice.

A

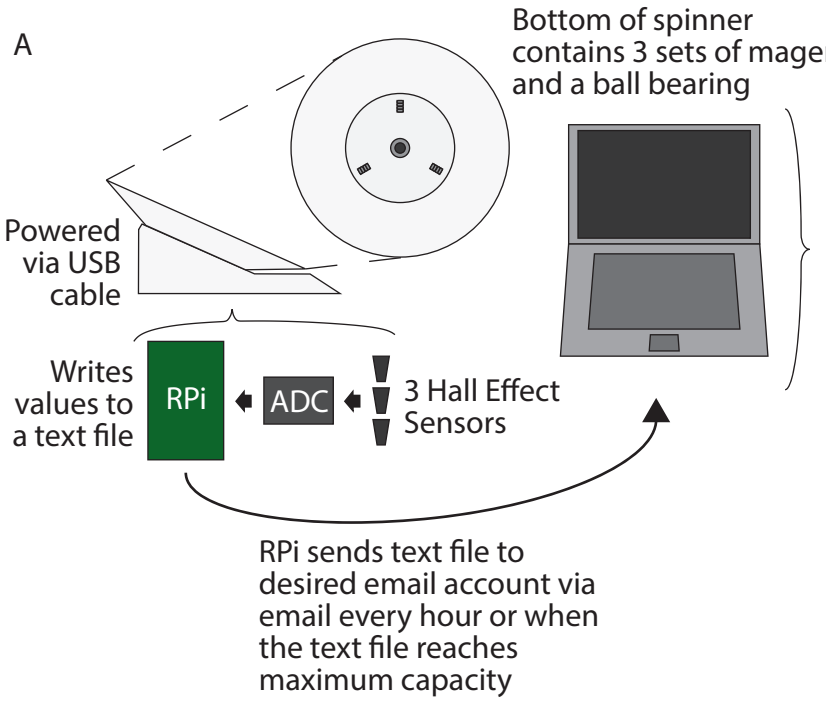

1. Using Python, text files are downloaded, and values are parsed from the text and saved in excel files.
2. Data is imported to MATLAB and stored in a MATLAB structure.
3. Distance and velocity are calculated, and the total distance and average velocity are plotted immediately.
4. Data in MATLAB structure can be analyzed using a script to look at whatever is of interest.

B

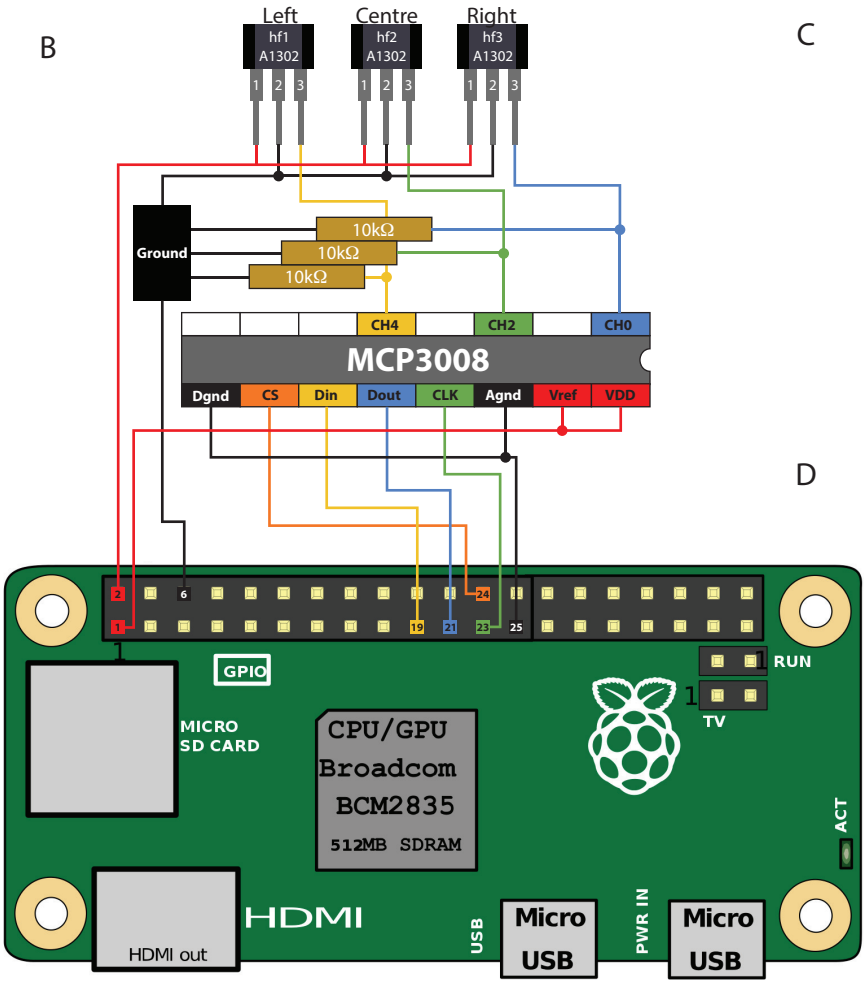

C

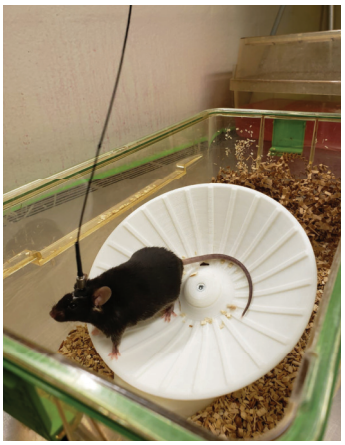

D

Figure 1

A

B

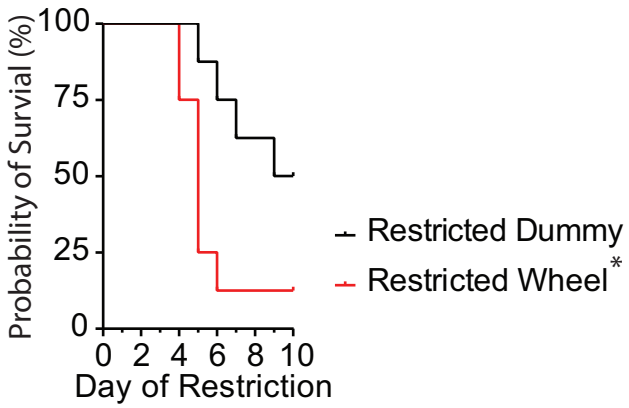

Figure 2

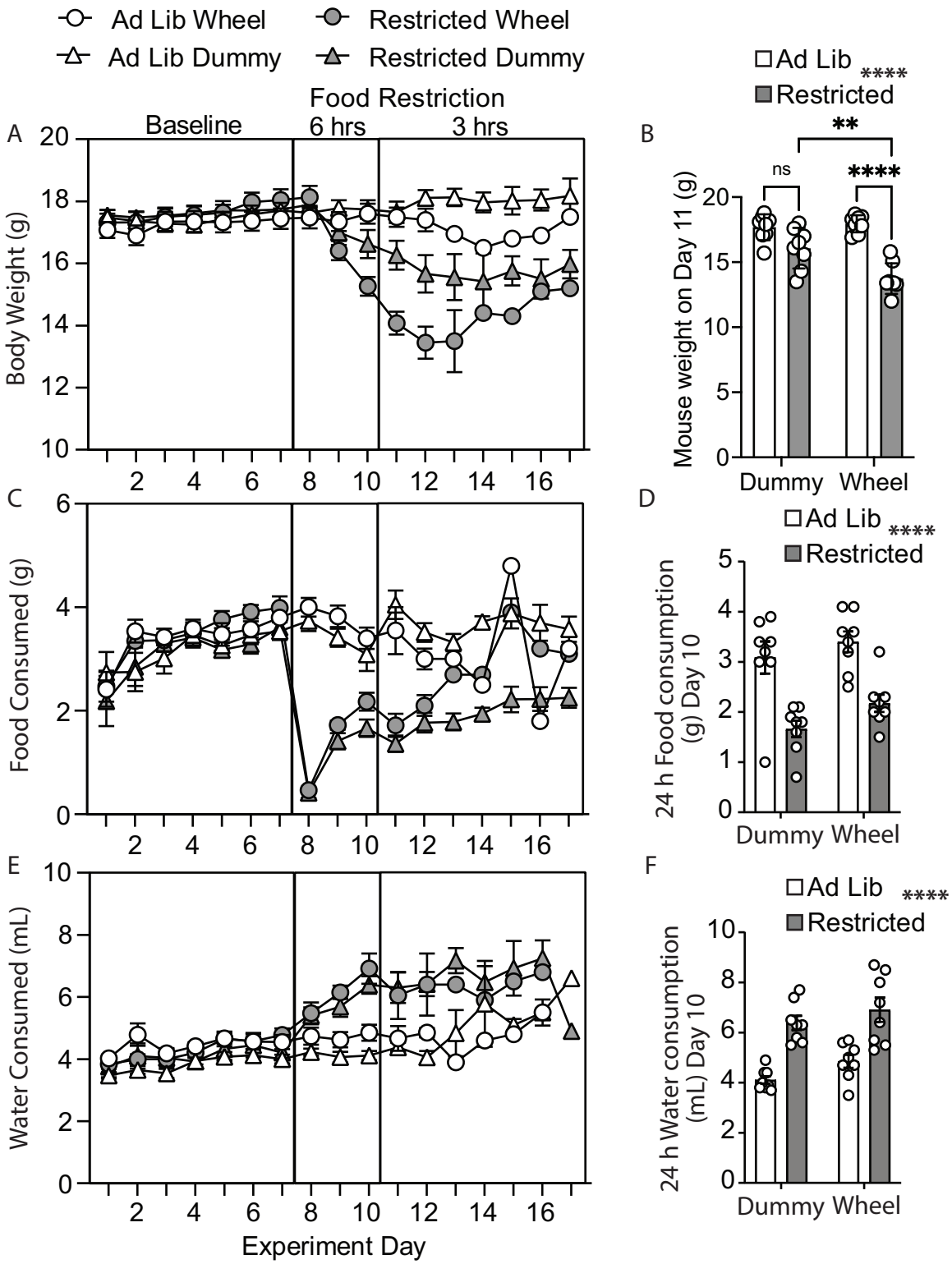

Figure 3

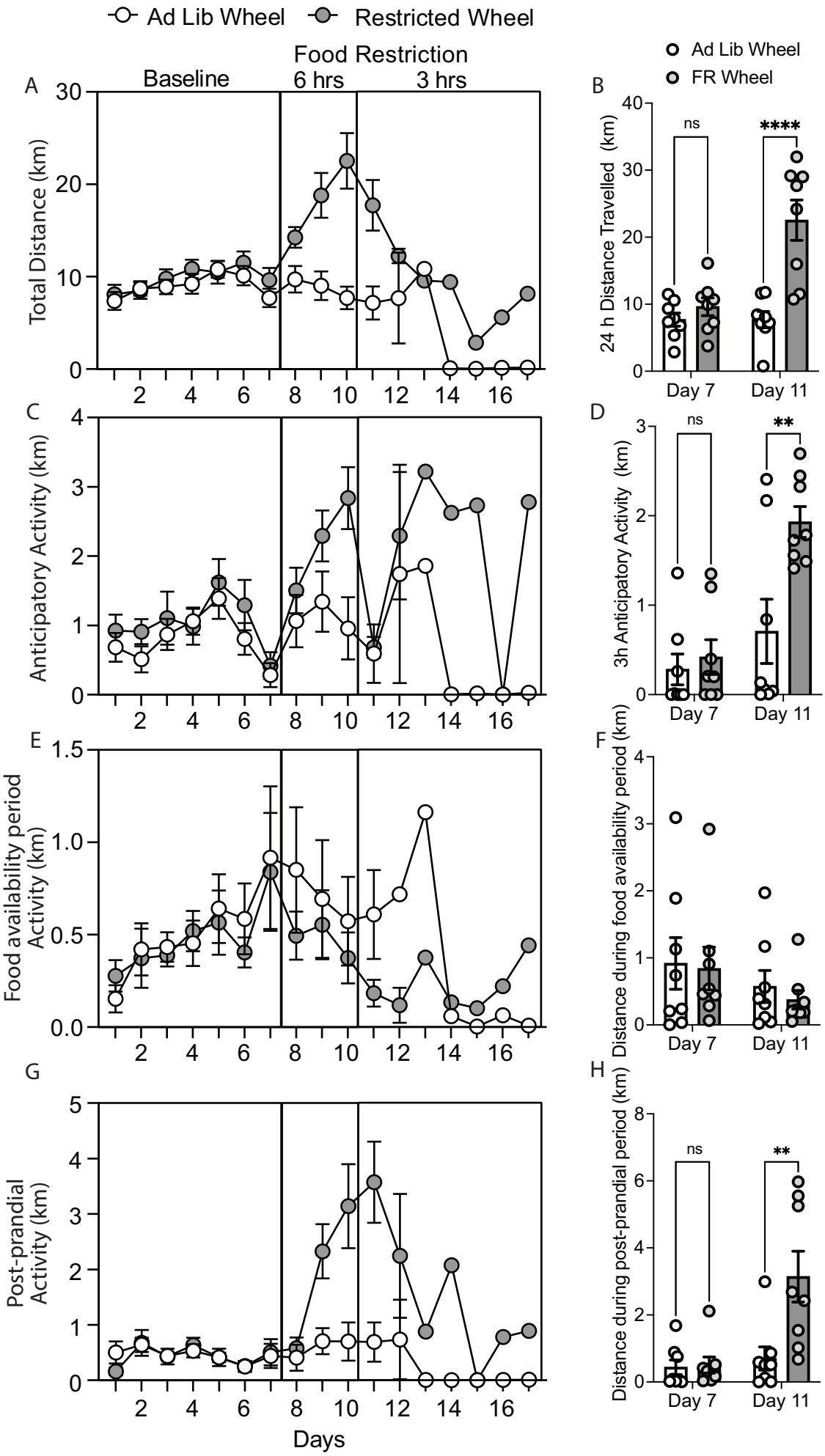

Figure 4

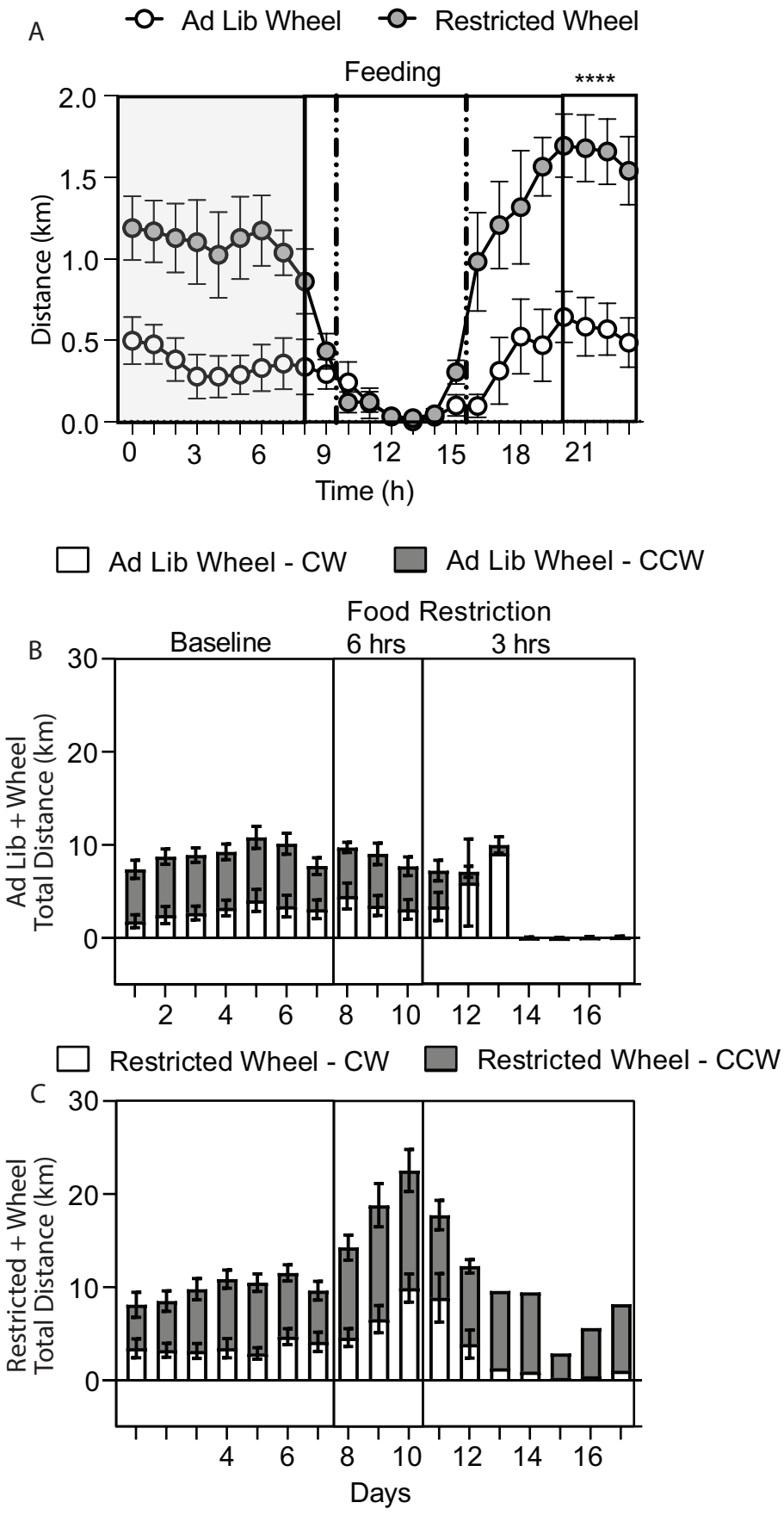

Figure 5

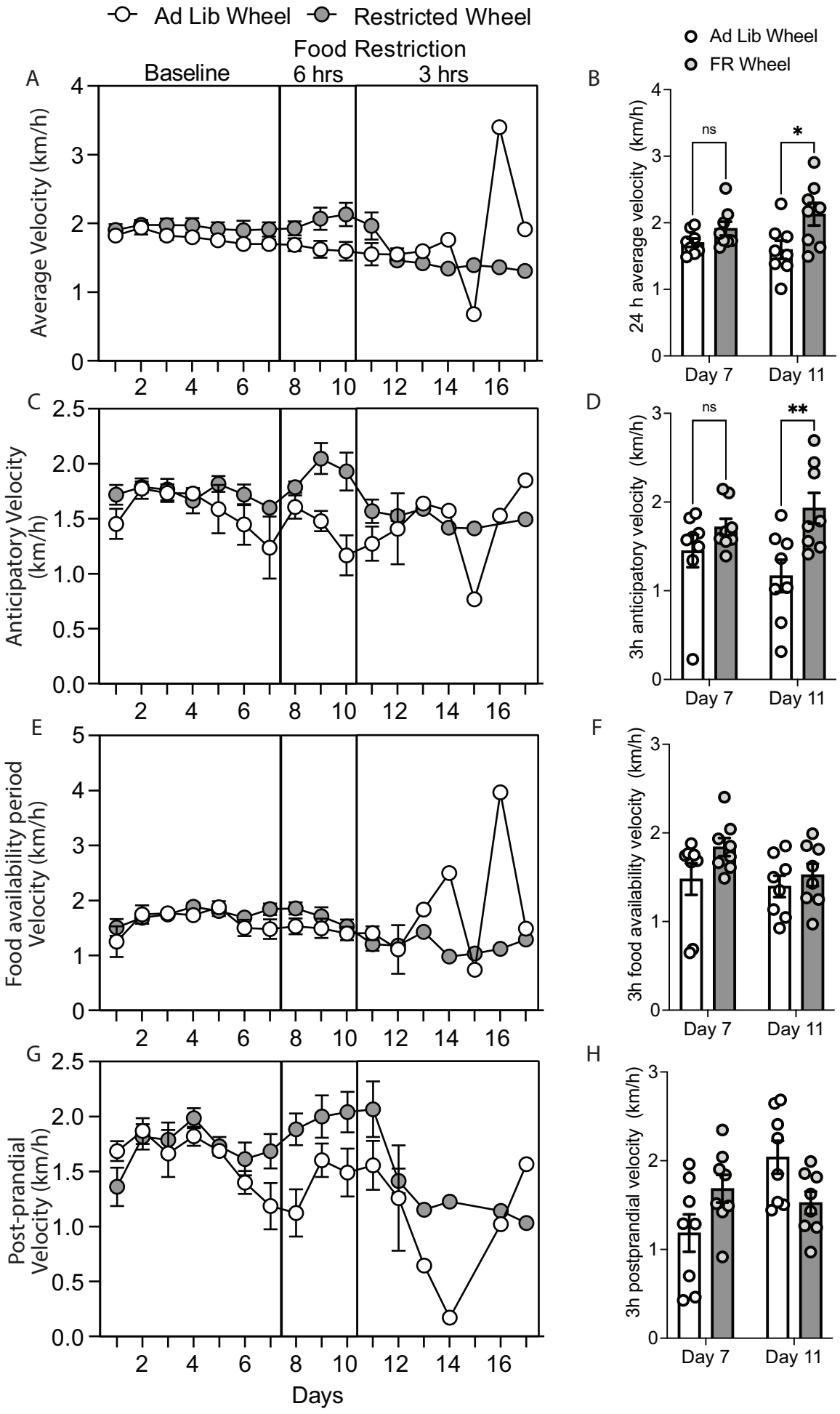

Figure 6